Structure of a Type IV Secretion System Core Complex

Rémi Fronzes,[1] Eva Schäfer,[1*] Luchun Wang,[1*] Helen R. Saibil,[1] Elena V. Orlova,[1] Gabriel Waksman[1,2]†

Type IV secretion systems (T4SSs) are important virulence factors used by Gram-negative bacterial pathogens to inject effectors into host cells or to spread plasmids harboring antibiotic resistance genes. We report the 15 angstrom resolution cryo–electron microscopy structure of the core complex of a T4SS. The core complex is composed of three proteins, each present in 14 copies and forming a ~1.1-megadalton two-chambered, double membrane–spanning channel. The structure is double-walled, with each component apparently spanning a large part of the channel. The complex is open on the cytoplasmic side and constricted on the extracellular side. Overall, the T4SS core complex structure is different in both architecture and composition from the other known double membrane–spanning secretion system that has been structurally characterized.

Type IV secretion systems (T4SSs) are macromolecular nanomachines utilized for the transport of proteins or DNA across the bacterial cell envelope of Gram-negative bacteria (*1*, *2*). The archetypal *Agrobacterium tumefaciens* T4SS comprises 12 proteins named VirB1through 11 and VirD4. T4SSs in other bacteria can display additional components or have homologs for only a subset of those proteins (*1*). T4SSs likely span the periplasm and both bacterial membranes. An extracellular pilus is associated with some T4SSs and is composed of a major (VirB2) and a minor (VirB5) subunit. Three adenosine triphosphatases (ATPases), VirB4, VirB11, and VirD4, are involved in substrate secretion and in system assembly. VirB6, VirB8, and VirB10 may form an inner membrane channel (*3*, *4*). At the outer membrane, the composition of the pore is unknown. The periplasmic protein VirB9 in complex with the short lipoprotein VirB7 could be part of this structure (*5*, *6*). However, no transmembrane region could be found or predicted in either protein. Moreover, VirB9 proteins share no sequence similarities with outer membrane secretins. Protein-protein interaction studies have identified a core T4SS complex consisting of four proteins, VirB7, 8, 9, and 10 (*1*, *7*). Together with VirB4, this T4SS core complex is the minimal functional entity (*8*, *9*). Here, we provide structural and functional insights on the equivalent core T4SS complex encoded by the plasmid pKM101.

The *virB7-10* gene cluster of the pKM101 plasmid was cloned and expressed (*10*). In this cluster, these genes are named *traN*, *traE*, *traO*, and *traF*, respectively. For clarity, each gene and protein will be named hereafter using both the Tra and VirB nomenclatures. Cloning of the *traN/virB7-traF/virB10* cluster introduced a Strep-tag at the C terminus (C-ST) of TraF/VirB10 (TraF/VirB10$_{C\text{-}ST}$) (fig. S1, A and B). Induction of gene expression, preparation of the membrane fraction followed by solubilization of membrane proteins, and a two-step purification procedure resulted in the purification of a complex containing TraN/VirB7, TraO/VirB9, and TraF/VirB10$_{C\text{-}ST}$ [the "wild-type core" complex (Fig. 1A) (*10*)]. TraE/VirB8 (although strongly expressed) was not present in the purified complex. The stoichiometry of the different components of the core complex was shown to be 1:1:1 (fig. S1C) (*10*). The core TraN/VirB7-TraO/VirB9-TraF/VirB10 complex purified as a ~1100-kD complex (Fig. 1B) (*10*). Wild-type core complexes were then visualized by negative-stain electron microscopy (EM) (*10*). We observed ringlike and multilayered particles, corresponding to end and side views of the complex, respectively (fig. S2A). Rotational symmetry analysis of end-view class averages revealed a clear 14-fold symmetry (fig. S2) (*10*). Thus, the T4SS core complex is formed of 14 copies each of three proteins.

The importance and role of TraN/VirB7 lipidation on core complex formation and localization were examined. TraN/VirB7 becomes acylated on Cys[15] (*11*). This residue was mutated to Ser (TraN$_{Cys15Ser}$) (fig. S3A), and the resulting *traN/virB7*$_{Cys15Ser}$*-traF/virB10*$_{C\text{-}ST}$ cluster was expressed (*10*). A complex (ΔL1) similar in size to the wild-type core complex was purified (fig. S3A). Thus, lipidation of TraN/VirB7 is not required for core complex formation. We next examined the membrane localization of the ΔL1 core complex and established that both the wild-type and ΔL1 core complexes reside in the inner membrane; however, only the wild-type core complex is found in the outer membrane (fig. S3A) (*10*). Thus, lipidation of TraN/VirB7 is required for targeting of the core complex to the outer membrane. This interpretation was confirmed by accessibility studies on whole cells (fig. S3B) (*10*). Finally, we investigated the role of each of the genes in the *traN/virB7-traF/virB10* cluster by deleting them one at a time and demonstrated that TraE/VirB8 is not involved in the assembly of the core complex but that TraN/VirB7, TraO/VirB9, and TraF/VirB10 are essential for the formation of the 14-oligomer ring complex (fig. S3) (*10*).

To obtain a detailed view of the three-dimensional (3D) structure of the TraN-TraO-TraF$_{C\text{-}ST}$ complex, a cryo–electron microscopy (cryo-EM) data set was collected and used to reconstruct a 15 Å resolution 3D map of the complex with 14-fold symmetry (fig. S4) (*10*). The final structure is shown in Fig. 2. The T4SS core complex has an overall dimension of 185 Å in both height and diameter (Fig. 2). It is made of two main layers, labeled inner (I) and outer (O) with reference to the orientation, which will be

[1]Institute of Structural and Molecular Biology, School of Crystallography, Birkbeck College, Malet Street, London, WC1E 7HX, UK. [2]Division of Biosciences, University College London, Gower Street, London, WC1E 6BT, UK.

*These authors contributed equally to this work.
†To whom correspondence should be addressed. E-mail: g.waksman@ucl.ac.uk, g.waksman@mail.cryst.bbk.ac.uk

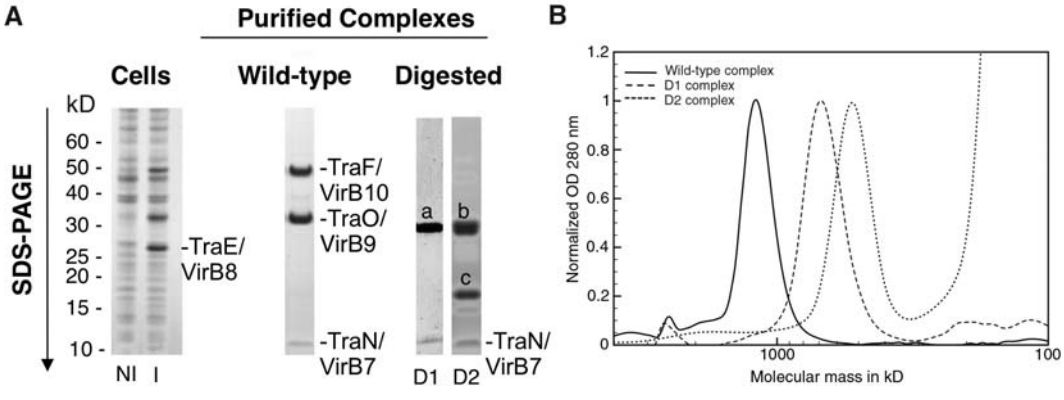

Fig. 1. Purification of the pKM101-encoded T4SS complex core. (**A**) SDS-polyacrylamide electrophoresis analysis of the noninduced (NI) and induced (I) cells (left), the pure wild-type core complex (middle), and digested D1 and D2 complexes (right). (Right) The top left band, a, contains a C-terminal fragment of TraF/VirB10 and full-length TraO/VirB9; the top right band, b, contains a C-terminal fragment of TraF/VirB10, and the middle band, c, which contains a C-terminal fragment of TraO/VirB9. The content of the a, b, and c bands was assessed by mass spectrometry and N-terminal sequencing. (**B**) Gel filtration of the wild-type, D1, and D2 complexes.

discussed later (Fig. 2A). Both layers are either in part (the I layer) or entirely (the O layer) composed of two walls (Fig. 2B).

The O layer consists of two regions: the cap, which is 110 Å in diameter and 40 Å high, and the main body, which is 185 Å in diameter and 60 Å high (Fig. 2A). In the cap, the internal wall forms a 20 Å hole that tapers off to a 10 Å diameter constriction at the main body (Fig. 2B). In the main body, the internal wall forms a chamber (Fig. 2B) that is 110 Å wide and 30 Å high. Internal protuberances are clearly visible at the bottom of the chamber; these leave a large opening of 55 Å.

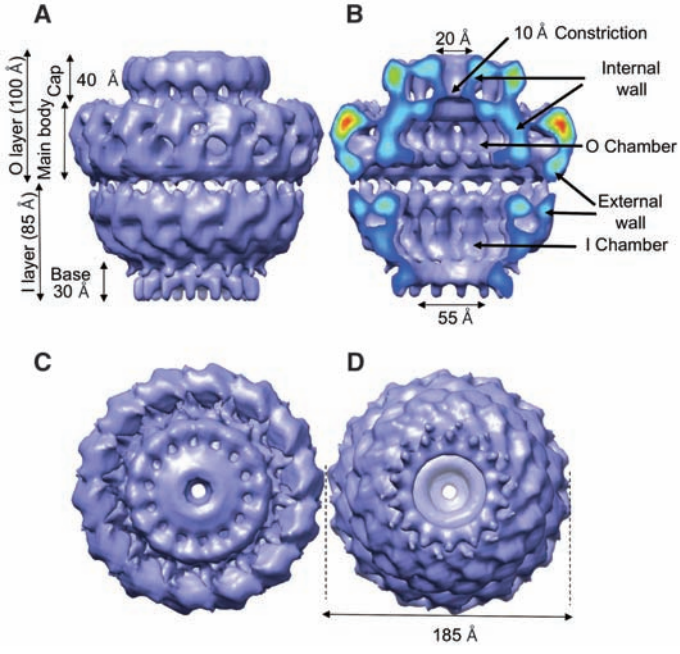

Fig. 2. Cryo-EM structure of the TraN/VirB7, TraO/VirB9, and TraF/VirB10$_{C\text{-}ST}$ core complex. (**A**) Side view. (**B**) Cutaway side view. Electron density is color-coded from red to blue to indicate regions of strong to weaker density, respectively. (**C**) Top view (view from outside the cell). (**D**) Bottom view (view from the cytoplasm). All features and dimensions mentioned in the text are indicated.

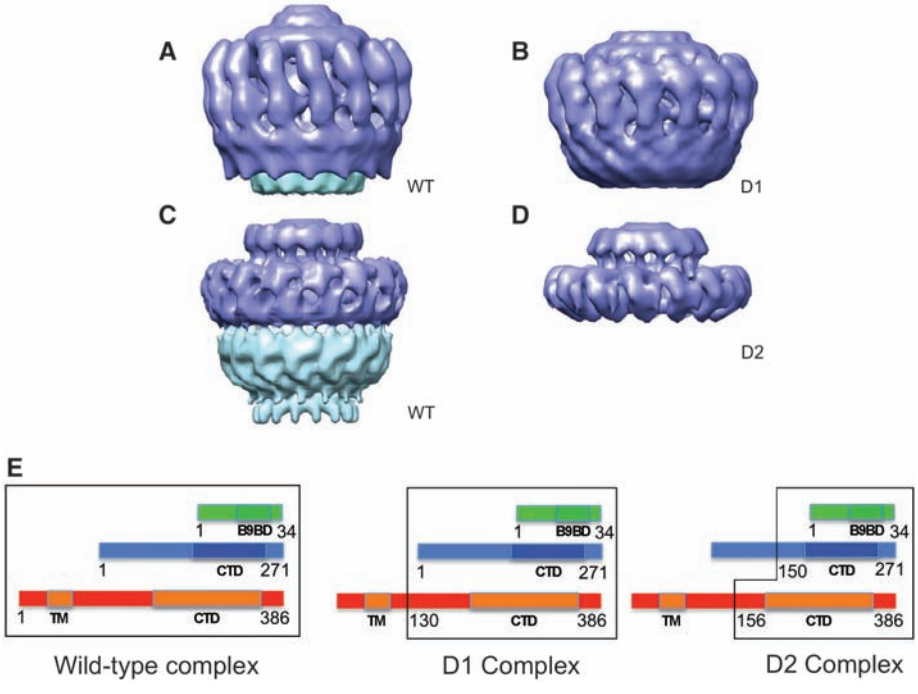

Fig. 3. Comparison of the structures of the wild-type complex, (**A**) and (**C**); D1, (**B**); and D2, (**D**); as revealed by negative-stain EM (A) and (B) and cryo-EM (C) and (D). Parts removed by proteolysis are shown in cyan. (**E**) Schematic diagrams of the composition of each of the complexes. TraN, TraO, and TraF are in the same representation and color-coding as in fig. S1A. Numbering for TraN and TraO are for the mature proteins (signal sequence excluded). A black outline encloses the parts of the proteins included in the various complexes.

The I layer resembles a cup. It is linked to the O layer by thin stretches of density. The two walls of the cup merge into a single wall near the base. The internal wall defines a chamber that is as wide as the chamber in the O layer, but double the height at 60 Å. This chamber tapers off at the bottom to a diameter of 55 Å, where it reaches the 30 Å high base from which 14 fingers of density extend downwards.

To locate specific proteins in the core complex, we used limited proteolysis followed by imaging of the resulting complexes by either negative-stain or cryo-EM (*10*). A limited proteolysis performed at low trypsin concentration (2 μg/ml) generated a first subcomplex (D1) of ~700 kD, where the residues 1 to 129 of TraF/VirB10 were removed from the core complex (Fig. 1). More extensive digestion with 2 mg/ml trypsin produced a second subcomplex of ~500 kD (D2) in which residues 1 to 155 of TraF/VirB10 and residues 1 to 149 of the mature TraO/VirB9 were removed (Fig. 1).

Both the D1 and D2 complexes were visualized using negative-stain, and a cryo-EM structure was determined for D2 (figs. S2 and S4). Particles in the D1 negative-stain and D2 negative-stain EM data sets exhibited clear 14-fold symmetry (fig. S2E). The only difference between the negative-stained wild-type and D1 complex structures is the disappearance of the base in the I layer, indicating that the base is made of the N terminus of TraF/VirB10 (Fig. 3, A and B). As this part of TraF/VirB10 is known to insert in the inner membrane, this observation was used to orient the complex and positioned the I layer toward the inner membrane and the O layer toward the outer membrane.

Comparison of the cryo-EM structures of the wild-type and D2 complexes (Fig. 3, C and D) demonstrates that the structure of the O layer in the wild-type core complex is similar to that of the D2 complex. Thus, given that the composition of the D2 complex is known (Fig. 1), we can conclude that the O layer is mainly composed of the C-terminal domain of TraF/VirB10 (TraF/VirB10$_{Cterm}$ residues 156 to 386), the C terminus of TraO/VirB9 (TraO/VirB9$_{Cterm}$ residues 150 to 271 of the mature protein), and TraN/VirB7 (Figs. 1 and 3E). Fourteen of each of these would give a mass of 602 kD, consistent with the complex mass calculated from the cryo-EM map (647 kD when the volume is calculated on the basis of a mass of 1050 kD for the whole structure). This implies that the I layer is composed of the N-terminal regions of TraF/VirB10 and TraO/VirB9, a conclusion also supported by the small difference between the wild-type and D1 negative-stain structures in the base region of the I layer.

To confirm the placement of the N terminus of TraF/VirB10 at or near the base of the I layer, a sequence encoding a His$_6$-tag was introduced at the 5′ end of the *traF/virB10* gene (resulting

in the *traN*-$_{N\text{-}His}$*traF*$_{C\text{-}ST}$ cluster) (*10*). The resulting core complex is similar to the wild-type complex. When incubated with His_6-specific antibodies and imaged using negative-stain EM (*10*), this complex shows clear additional electron density in the vicinity of the base of the I layer in both the raw data and class averages (Fig. 4A).

From the known data, the most likely region of the O layer to insert in the outer membrane is the C-terminal domain of TraO/VirB9 (*12*). The structure of this domain bound to TraN/VirB7 (*12*) shows a three-stranded β appendage in TraO, which loosely associates with the TraO β barrel. This β appendage was hypothesized to undergo a large conformational change to protrude out of the cell (*12*). It is likely that the structure adopted by this region of the TraO/VirB9 C-terminal domain forms one of the two walls in the cap region of the O layer, which suggests that the cap is inserted in the outer membrane. Thus, the O and I chambers likely form a periplasmic channel, which extends over a distance of 105 Å, a distance comparable to that observed in the WzA/WzC complex, where the two transmembrane regions are 100 Å apart (*13*) (fig. S5B).

The known structure of the C-terminal domain of the ComB10 protein (a structural prototype for C-terminal domains of VirB10 homologs) was fitted into the electron density of the external wall of the O layer's main body, with its N terminus directed toward the I layer (fig. S5D) (*10*, *14*). The rationale for locating the structure in that region is threefold: (i) in terms of shape complementarity, this is the only part of the O-layer electron density where the structure can fit; (ii) the goodness-of-fit parameter is high [0.48 as determined by SITUS (*15*)]; (iii) this external wall of the O layer is not accessible to the substrate, and it has been shown that, in *A. tumefaciens*, the substrate does not contact VirB10 directly during transfer (*16*). In the proposed location, VirB10 would be in an ideal position to play its role of energy transducer that has been characterized in the *A. tumefaciens* T4SS. In *A. tumefaciens*, VirB10 undergoes a conformational change induced by the inner membrane ATPases and the presence of adenosine triphosphate, a conformational change that is required to bring VirB9 and VirB10 together and to activate the T4SS (*17*). Clearly, in the pKM101 T4SS, the ATPases are not required to bring the two proteins together because the core complex forms spontaneously in the presence of the three core proteins TraN/VirB7, TraO/VirB9, and TraF/VirB10; however, they may be necessary for activation of the machinery. We suggest that ATPase function (perhaps together with VirB6 and VirB8) at the inner membrane induces conformational changes in the C-terminal domain of VirB10 that results in the opening of the constriction in the cap, which is required to allow passage of nucleoprotein complexes.

Our interpretation of the data presented here can be summarized in a model in which TraF/VirB10 forms the major part of the outer surface of the core complex (except the cap), whereas TraO/VirB9 together with TraN/VirB7 form the internal walls of the core complex. In that configuration, TraF/VirB10 would not directly take part in substrate transfer, but would play a role in reshaping the inner TraO surface to allow passage of the substrate through the O-layer cap (Fig. 4B).

The structure of the core T4SS machinery presented here is different from that of the type III secretion system (T3SS) (*18*) (fig. S5C). Indeed, the components of the two systems share no sequence similarity, and the envisaged multimerization order of each component is different. T4SSs have likely evolved the architecture revealed here in order to secrete a wide variety of substrates including large DNA-protein complexes.

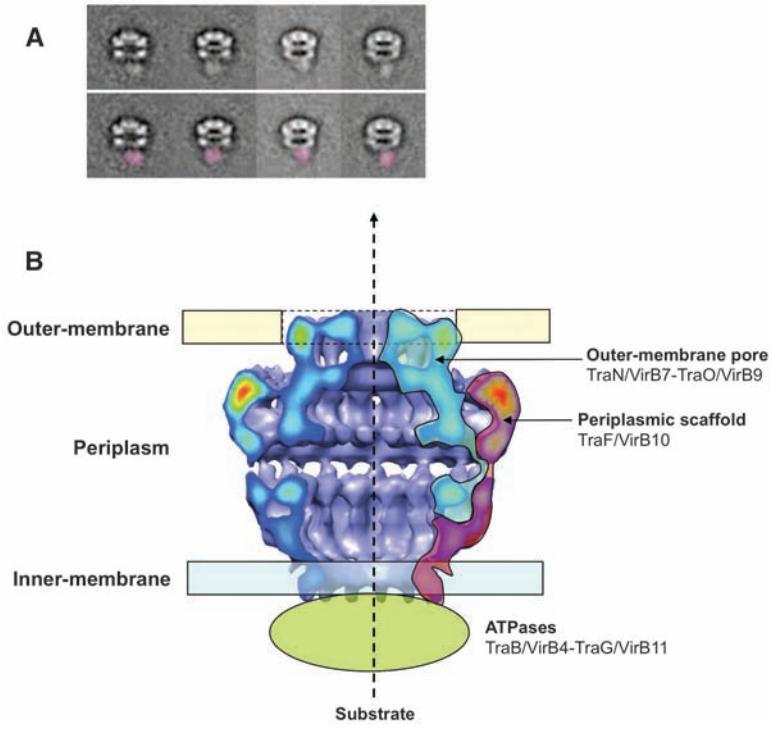

Fig. 4. Localization of core complex macromolecular components to the various regions of the cryo-EM structure. (**A**) Immunolocalization of the N terminus of TraF/VirB10 by negative-stain EM. Representative class averages are shown, with (bottom) additional density due to His_6–specific antibodies colored in red. (**B**) Localization of TraO/VirB9 (blue) and TraF/VirB10 (red) within the cryo-EM structure of the wild-type core complex.

References and Notes

1. P. J. Christie, K. Atmakuri, V. Krishnamoorthy, S. Jakubowski, E. Cascales, *Annu. Rev. Microbiol.* **59**, 451 (2005).
2. G. Schroder, E. Lanka, *Plasmid* **54**, 1 (2005).
3. L. Krall *et al.*, *Proc. Natl. Acad. Sci. U.S.A.* **99**, 11405 (2002).
4. D. V. Ward, O. Draper, J. R. Zupan, P. C. Zambryski, *Proc. Natl. Acad. Sci. U.S.A.* **99**, 11493 (2002).
5. S. J. Jakubowski, E. Cascales, V. Krishnamoorthy, P. J. Christie, *J. Bacteriol.* **187**, 3486 (2005).
6. C. Baron, Y. R. Thorstenson, P. C. Zambryski, *J. Bacteriol.* **179**, 1211 (1997).
7. A. Das, Y. H. Xie, *J. Bacteriol.* **182**, 758 (2000).
8. Z. Liu, A. N. Binns, *J. Bacteriol.* **185**, 3259 (2003).
9. R. L. Harris, V. Hombs, P. M. Silverman, *Mol. Microbiol.* **42**, 757 (2001).
10. Materials and methods, supporting text, and figures are available as supporting materials on *Science* Online.
11. D. Fernandez *et al.*, *J. Bacteriol.* **178**, 3156 (1996).
12. R. Bayliss *et al.*, *Proc. Natl. Acad. Sci. U.S.A.* **104**, 1673 (2007).
13. R. F. Collins *et al.*, *Proc. Natl. Acad. Sci. U.S.A.* **104**, 2390 (2007).
14. L. Terradot *et al.*, *Proc. Natl. Acad. Sci. U.S.A.* **102**, 4596 (2005).
15. W. Wriggers, R. A. Milligan, J. A. McCammon, *J. Struct. Biol.* **125**, 185 (1999).
16. E. Cascales, P. J. Christie, *Science* **304**, 1170 (2004).
17. E. Cascales, P. J. Christie, *Proc. Natl. Acad. Sci. U.S.A.* **101**, 17228 (2004).
18. T. C. Marlovits *et al.*, *Science* **306**, 1040 (2004).

19. This work was funded by research grants from the Wellcome Trust to G.W. and UK Biotechnology and Biological Sciences Research Council to H.R.S. and by an equipment grant from the Wellcome Trust to H.R.S and E.V.O. Also, H.R.S. and E.V.O. thank the European Union Network of Excellence in Three-Dimensional Electron Microscopy (3DEM) for support. EM maps have been deposited to the EM data bank under the entry codes EMD-5031 to EMD5035 for cryo-EM wild-type, negative-stain EM wild-type, negative-stain EM D1, cryo-EM D2, and negative-stain ΔL2 complexes, respectively.

Supporting Online Material

www.sciencemag.org/cgi/content/full/323/5911/266/DC1
Materials and Methods
Figs. S1 to S6
Table S1
References

18 September 2008; accepted 14 November 2008
10.1126/science.1166101